Finite Element Modelling of Post-Tensioned Timber Beam-Column Joints Designed for Seismic Loading

Ahmad Rahmzadeh [1], Asif Iqbal [2]

[1] PhD Student, School of Engineering, The University of British Columbia, Kelowna, BC V1V 1V7, Canada.
[2] Assistant Professor, Integrated Wood Design, University of Northern British Columbia, Prince George, BC V2N 4Z9, Canada.

ABSTRACT

As a part of sustainable development initiatives, post-tensioned timber structural systems have been developed in recent years with the intention of implementation in seismically active regions. Ductility is achieved through rocking connections between members and optional steel yielding elements. Numerical investigations on such systems have been mostly limited to macro-modeling to avoid complexities arising from the wood anisotropy. This paper examines the lateral cyclic behavior of post-tensioned Laminated Veneer Lumber (LVL) beam-column subassemblies using three-dimensional continuum finite element (FE) modeling. The results of a testing program on full-scale interior joints with unreinforced and steel reinforced configurations at the connection interface are presented. A description of the pre-processing and solution of the FE models, including material, geometric and contact nonlinearities, element mesh, and analysis is provided. The FE results are then validated against the experiments through a verification study. Focus is placed upon the anisotropy of the material as well as the difficulties emerging from performing the nonlinear analysis for such systems.

Keywords: Laminated Veneer Lumber, Post-tensioned connection, Finite element, Anisotropic material, Nonlinear analysis.

INTRODUCTION

In an attempt to introduce mass timber as an eco-friendly alternative to concrete and steel in seismically active regions, posttensioning technique was extended to timber-based structural systems. In these structural systems structural members made of engineered wood products are assembled and tied together using conventional post-tensioning. When the system is subject to lateral loading, strain is limited due to gap opening at the rocking connection interface and ductility can be achieved using this technique even though timber is a brittle material. The posttensioning provides self-centering ability to the system and the structural members are protected against damage and energy dissipation within the members is relatively low which might lead to considerable lateral deformations during a seismic event. Henceforth, when additional energy dissipation is deemed necessary, sacrificial mild steel elements are used to enhance the energy dissipation capacities of these systems. The most common type of energy dissipation elements are essentially small-sized buckling resistant braces with steel bars encased by steel tubes and the gaps between the bars and the casing filled by epoxy. The elements are placed across joint interfaces and connected to separate members at the two ends. They are loaded axially during the rocking motion between the two members at the joint interface and energy is dissipated through the yielding of mild steel in axial tension and compression.

This paper studies the lateral cyclic behavior of post-tensioned LVL beam-column joints using 3D continuum finite element (FE) modeling. The results of a testing program on full-scale interior joints with unreinforced and steel reinforced configurations at the connection interface are presented. A description of FE modeling and solution procedure, including material, geometric and contact nonlinearities, element mesh, and analysis is provided. The FE results are then validated against the experiments through a verification study with a focus on the anisotropy of timber along with the complications arising out of performing the nonlinear analysis for such systems.

DESCRIPTION OF TEST SPECIMENS

The full-scale beam-column joint was adopted from an alternative solution using post-tensioned LVL members to a six-story conventional reinforced concrete building constructed in a moderately seismic region [1]. Bay spacing and interstorey height of the considered frame were 6000 mm and 3200 mm, respectively. The beams were post-tensioned using twelve 12.7 mm diameter seven-wire strands. Threaded bars were epoxied to the beams and column to anchor the energy dissipaters and their steel brackets. The test setup and member dimensions are demonstrated in Figure 1.
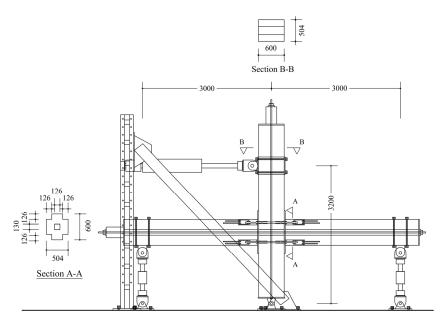
Figure 1. Test setup.

Several specimens were tested to investigate the effect of various parameters including the initial posttensioning stress ($f_{pt,0}$), reinforcing the rocking interface, and buckling-restraint energy dissipaters. Details of the specimens are given in Table 1. An axial force of 900 kN was applied on the column by vertical tendons to mimic the gravity load. The quasi-static lateral loading protocol consists of two-cycle interstorey drifts with an increment of 0.5%. Details of the experimental program and outcomes can be found in Ref. [2].

Table 1. Properties of specimens.

Specimen	$f_{pt,0}/f_y^*$	Reinforcing plate	Energy dissipater
8	30%	30 mm	-
9	55%	30 mm	-
10	55%	30 mm	8-16[**] mm
14	58%	-	-

[*] Yield stress of the strand.

[**] Eight energy dissipaters with 16 mm diameter in the fuse length.

FE MODELING PROCEDURE

In an anisotropic material, the material properties are different in dissimilar orientations since there is no planes of material property symmetry. The stiffness matrix of such a material has 36 constants with 21 independent constants if the characteristics of the strain energy are taken into account. The timber material can be assumed as orthotropic wherein the properties are different in three mutually perpendicular directions. Due to material property symmetry, the number of independent elastic constants for this material reduces to nine having no shear-extension and shear-shear couplings. The flexibility or compliance matrix, which is the inverse of the stiffness matrix, for an orthotropic material is as follows [3],

$$\mathbf{S} = \begin{bmatrix} \dfrac{1}{E_x} & -\dfrac{\nu_{xy}}{E_x} & -\dfrac{\nu_{xz}}{E_x} & 0 & 0 & 0 \\[2ex] & \dfrac{1}{E_y} & -\dfrac{\nu_{yz}}{E_y} & 0 & 0 & 0 \\[2ex] & & \dfrac{1}{E_z} & 0 & 0 & 0 \\[2ex] & & & \dfrac{1}{G_{xy}} & 0 & 0 \\[2ex] & & & & \dfrac{1}{G_{yz}} & 0 \\[2ex] & & & & & \dfrac{1}{G_{xz}} \end{bmatrix} \tag{1}$$

in which, E_x, E_y and E_z are Young's moduli in the x, y and z directions, respectively, and ν_{xy}, ν_{xz} and ν_{yz} are major Poisson's ratios, and G_{xy}, G_{yz} and G_{xz} are shear moduli in the x-y, y-z and x-z planes, respectively. Minor Poisson's ratios can be obtained by using three reciprocal relations stemming from the symmetry of the above matrix. In order to avoid negative strain energy, the matrix must be positive-definite. Such a thermodynamic requirement is satisfied by the following equations [4],

$$\left(1 - \nu_{yz}\nu_{zy}\right), \left(1 - \nu_{xz}\nu_{zx}\right), \left(1 - \nu_{xy}\nu_{yx}\right) > 0 \tag{2}$$

$$1 - \nu_{xy}\nu_{yx} - \nu_{yz}\nu_{zy} - \nu_{xz}\nu_{zx} - 2\nu_{xy}\nu_{yz}\nu_{zx} > 0 \tag{3}$$

Assuming that the mechanical properties of timber in the perpendicular plane to the grain are equal (transversely isotropic), the stiffness matrix can be further simplified to a matrix with five independent constants. For such a case, if the grain is considered to be along the x direction, y and z subscripts are interchangeable in Eqs. (1-3) since y-z is the isotropic plane.

The averaged apparent Young's modulus and strength of LVL produced by the same manufacturer as the tested beam-column connections were experimentally investigated by Newcombe [5]. A Young's modulus of 8000 MPa and 300 MPa and a compressive strength of 44 MPa and 12.5 MPa were obtained for the directions parallel and perpendicular to the grain, respectively. The shear moduli in the planes containing the grain direction and in the isotropic plane were considered as 510 MPa and 32 MPa, respectively. Also, a shear strength of 5.3 MPa was used [6]. Major Poisson's ratios ν_{xy}, ν_{xz} and ν_{yz} were adopted from Ref. [7] as 0.38, 0.51 and 0.51, respectively.

Under compression, a defect-free timber shows a strain-stress behavior in the grain direction similar to that of concrete. However, in the perpendicular to the grain the behavior is approximately bilinear with no distinct ultimate strength due to continuous increase of the stress following the elastic region. The corresponding behaviors under tension are brittle fracture and splitting failure [6]. In this study, the behavior parallel and perpendicular to the grain was modeled as elastic-perfectly plastic. Although it might seem that this modeling approach is not realistic in the grain direction, it can be justified by the fact that the beam and column were designed so that they would remain elastic. The tests showed that the beam and column did not experience significant damages in the parallel to the grain direction, suggesting that the strength degradation was negligible.

In order to predict the nonlinear behavior of timber, a yield criterion capable of capturing the anisotropy of the material is needed. The quadratic form of Hill's criterion which is an extension of the von Mises yield criterion is well suited for this purpose. Based on this criterion, for an anisotropy with three mutually orthogonal plane of symmetry, yielding under multiaxial stress state occurs once the following equation is satisfied [8],

$$F\left(\sigma_{yy} - \sigma_{zz}\right)^2 + G\left(\sigma_{zz} - \sigma_{xx}\right)^2 + H\left(\sigma_{xx} - \sigma_{yy}\right)^2 + 2L\tau_{yz}^2 + 2M\tau_{zx}^2 + 2N\tau_{xy}^2 = 1 \tag{4}$$

in which, σ_{ij} are stresses when the principal directions of anisotropy are the reference axes, and F, G, H, L, M and N are material constants which are defined as follows,

$$F = \frac{1}{2}\left(\frac{1}{\sigma_{yy}^{y\,2}} + \frac{1}{\sigma_{zz}^{y\,2}} - \frac{1}{\sigma_{xx}^{y\,2}}\right) \qquad\qquad L = \frac{1}{2\tau_{yz}^{y\,2}}$$

$$G = \frac{1}{2}\left(\frac{1}{\sigma_{zz}^{y\,2}} + \frac{1}{\sigma_{xx}^{y\,2}} - \frac{1}{\sigma_{yy}^{y\,2}}\right) \qquad\qquad M = \frac{1}{2\tau_{zx}^{y\,2}} \qquad\qquad (5)$$

$$H = \frac{1}{2}\left(\frac{1}{\sigma_{xx}^{y\,2}} + \frac{1}{\sigma_{yy}^{y\,2}} - \frac{1}{\sigma_{zz}^{y\,2}}\right) \qquad\qquad N = \frac{1}{2\tau_{xy}^{y\,2}}$$

where, σ_{ij}^{y} ($i{=}j$) are yield stresses in the principal axes of anisotropy and σ_{ij}^{y} ($i{\neq}j$) are yield stresses in shear with respect to the principal axes of anisotropy.

Since the behavior of the energy dissipaters greatly affects that of the beam-column subassembly, a realistic material model should be chosen for the fused bar. The Chaboche kinematic hardening model with three back stresses was selected for that aim. Detailed explanation of simulation and calibration of such energy dissipaters can be found in Ref. [9]. A trilinear kinematic model with a strain-hardening ratio of 5% and a cutoff value at the ultimate strength was chosen for the strands. The modulus of elasticity and tensile strength of the strands, in accordance to ASTM 416 [10], are 199 GPa and 1860 MPa for Grade 270, respectively. The yield strength of the strands was assumed to be 80% of their tensile strength. For other steel materials including the reinforcing and anchor plates, internally threaded bars and brackets for energy dissipaters, a bilinear kinematic model with a strain-hardening ratio of 2% was used.

To simulate the cyclic behavior of the specimens, continuum FE models were generated using ANSYS Mechanical APDL [11]. The 3D SOLID185 brick element was employed to mesh the volumes. To model contacts, four-node surface-to-surface CONTA173 element was used. TARGE170 elements were used to specify target surfaces. Based on the tangential and normal characteristics of the surfaces, the contact behavior between various components was set either to Standard or Bonded. PRETS179 elements were utilized to create pretension sections in the strands and apply the posttensioning forces. The mesh density was selected based on a preliminary mesh sensitivity analysis. The developed FE model is illustrated in Figure 2.
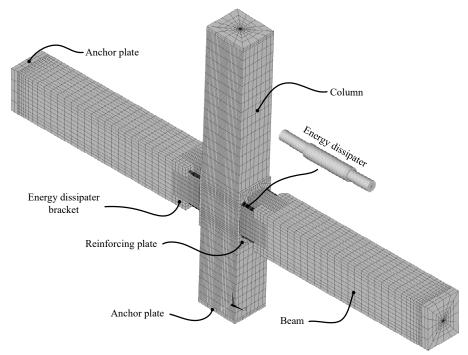

Figure 2. FE model of post-tensioned beam-column joint.

The boundary conditions were applied at the points of contra-flexure as the tests. In order to do so, the nodes of the beams at a distance of 3000 mm to the centerline of the column were constrained in the y direction. Also, to simulate the pin support of the column, the nodes on the centerline of bottom anchor plate were fixed in the x and y directions. The sequence of loading was modeled similar to that of the tests. First, the column was prestressed using vertical tendons, then the beams pre-compressed to the column, and finally the lateral displacements were applied at a height of 3200 mm from the column support.

Since the material, geometric and contact nonlinearities are present in these models, a nonlinear solver should be employed. In such cases, ANSYS [11] uses the Newton-Raphson approach in which the load is subdivided into a series of load increments that are applied over several load steps. The stiffness matrices are updated in each equilibrium iteration and are usually symmetric unless the frictional contacts are involved. ANSYS [11] utilizes a symmetrization algorithm to address such problems, however, it might lead to convergence issues if the frictional stresses are highly solution dependent. Hence, the unsymmetric solution option was selected to enhance the convergence even though it is more computationally expensive.

In the generated FE models, the rigid body motion is probable since some of the components are held together by frictional contacts. In order to prevent such an erroneous outcome, an initial extra step with small solution increments was defined in which all the components were constrained. In the following step and once the contacts between the members were established, the constraints were removed and the actual loading as the test was imposed.
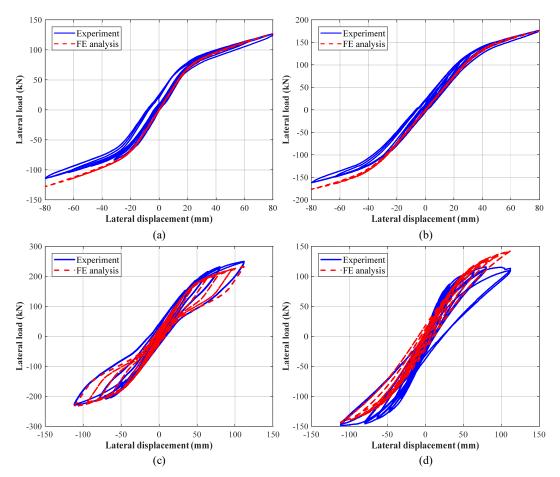

Figure 3. Experimental and FE load-displacement responses of: (a) specimen 8, (b) specimen 9, (c) specimen 10, and (d) specimen 14.

Comparison of the hysteresis responses obtained from the tests and FE analyses are shown in Figure 3. The initial stiffness is dependent on the member dimensions and elastic properties of the material. The FE models were able to predict the initial stiffness very well. Increasing the initial posttensioning force increases the decompression force and following that the lateral load capacity for a given drift. This can be concluded from the comparison of the responses in Figure 3(a-b). Gap opening/closing was well captured by the FE models. As a result, the energy dissipaters were activated and dissipated energy as inferred by Figure 3(c) and shown in Figure 4. A more reliable way of evaluating the capability of the FE model in reproducing the gap opening/closing mechanism is comparing the amount of force in the strands throughout the cycles in the analysis with that of the test (Figure 5). The difference between the test and FE results for specimen 9 can be attributed to the non-uniformity of the timber material as well as the simplified elastic-perfectly plastic material model used.
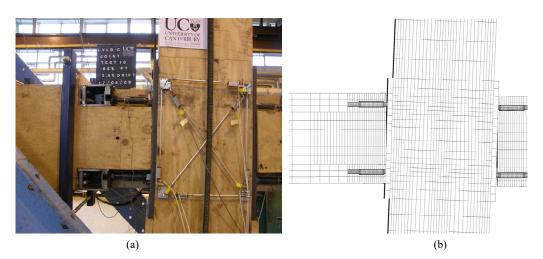
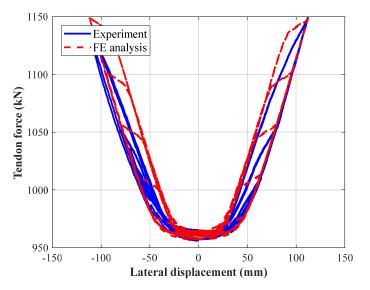Figure 4. Specimen 10 at the largest drift: (a) Test, (b) FE simulation.

Figure 5. Strand force of specimen 10.

CONCLUSIONS

The lateral cyclic behavior of internal post-tensioned LVL beam-column joints was studied in this paper. It was experimentally demonstrated that steel reinforcing the connection interface can significantly reduce damage and enhance the re-centering ability. A higher lateral load capacity can be achieved by increasing the initial posttensioning force and/or using energy dissipaters. The full capacity of the energy dissipating steel bars in both tension and compression was developed and the premature failure of the load transferring mechanism was avoided with the used configuration. A discussion was presented on the anisotropic behavior of timber. Simplifying assumptions were made to remove the complexities of the FE modeling of timber. Comparison of the test and FE results showed that such assumptions did not affect the results significantly. Other difficulties of FE modeling of such systems were briefly discussed. The numerical–experimental validations showed the viability of the FE models in predicting the behavior of these systems and further parametric investigations.

ACKNOWLEDGMENTS

REFERENCES

[1] Smith, T., Pampanin, S., Fragiacomo, M., Buchanan, A. (2008). "Design and Construction of Prestressed Timber Buildings for Seismic Areas." *Proceedings of the 10th World Conference on Timber Engineering*, Miyazaki, Japan.

[2]   Iqbal, A., Pampanin, S., Buchanan, A. H. (2016). "Seismic Performance of Full-Scale Post-Tensioned Timber Beam-Column Connections." *Journal of Earthquake Engineering*, 20(3), 383-405.

[3]   Tsai, S. W. (1966). *Mechanics of Composite Materials- Part Ii: Theoretical Aspects*. Air Force Materials Laboratory, Research and Technology Division, Air Force Systems Command.

[4]   Lempriere, B. M. (1968). "Poisson's Ratio in Orthotropic Materials." *AIAA Journal*, 6(11), 2226-7.

[5]   Newcombe, M. (2007). *Seismic Design of Multistorey Post-Tensioned Timber Buildings*, University of Pavia.

[6]   Buchanan, A. (2007). *Timber Design Guide*. 3rd ed. New Zealand Timber Industry Federation. Wellington, N.Z.

[7]   Schoenmakers, D. (2010). *Fracture and Failure Mechanisms in Timber Loaded Perpendicular to Grain by Mechanical Connections*, University of Eindhoven.

[8]   Hill, R. (1998). *The Mathematical Theory of Plasticity*. Clarendon Press.

[9]   Rahmzadeh, A., Iqbal, A. (2018). "Study of Replaceable Energy Dissipators for Self-Centering Structures." *Proceedings of the 11th National Conference in Earthquake Engineering*, Earthquake Engineering Research Institute, Los Angeles, CA.

[10]   ASTM. (2017). *Standard Specification for Low-Relaxation, Seven-Wire Steel Strand for Prestressed Concrete*. ASTM International. West Conshohocken, PA.

[11]   ANSYS. (2017). Ansys Multiphysics V18.2. ANSYS Inc. Canonsburg, PA.